The Plant Cell, Vol. 14, 1133–1146, May 2002, www.plantcell.org © 2002 American Society of Plant Biologists

Physical and Functional Interaction of the Arabidopsis K^+ Channel AKT2 and Phosphatase AtPP2CA

Isabelle Chérel,[1] Erwan Michard, Nadine Platet, Karine Mouline, Carine Alcon, Hervé Sentenac, and Jean-Baptiste Thibaud

Laboratoire de Biochimie et Physiologie Moléculaire des Plantes, Unité Mixte de Recherche 5004 Agro-M/Centre National de la Recherche Scientifique/Institut National de la Recherche Agronomique/Université Montpellier II, Place Viala, 34060 Montpellier Cedex 1, France

The AKT2 K^+ channel is endowed with unique functional properties, being the only weak inward rectifier characterized to date in Arabidopsis. The gene is expressed widely, mainly in the phloem but also at lower levels in leaf epiderm, mesophyll, and guard cells. The *AKT2* mRNA level is upregulated by abscisic acid. By screening a two-hybrid cDNA library, we isolated a protein phosphatase 2C (AtPP2CA) involved in abscisic acid signaling as a putative partner of AKT2. We further confirmed the interaction by in vitro binding studies. The expression of *AtPP2CA* (β-glucuronidase reporter gene) displayed a pattern largely overlapping that of *AKT2* and was upregulated by abscisic acid. Coexpression of AtPP2CA with AKT2 in COS cells and *Xenopus laevis* oocytes was found to induce both an inhibition of the AKT2 current and an increase of the channel inward rectification. Site-directed mutagenesis and pharmacological analysis revealed that this functional interaction involves AtPP2CA phosphatase activity. Regulation of AKT2 activity by AtPP2CA in planta could allow the control of K^+ transport and membrane polarization during stress situations.

INTRODUCTION

Potassium is the most abundant cation in the cytoplasm of the living cell, where it is involved in the regulation of ionic strength, osmotic potential, and membrane polarization. K^+ channels of the so-called Shaker family (nine genes in Arabidopsis) have been shown to play a role in K^+ uptake by the root periphery (AKT1: Lagarde et al., 1996; Hirsch et al., 1998), K^+ secretion into the root xylem sap (SKOR: Gaymard et al., 1998), K^+ transport in the phloem tissues (AKT2: Marten et al., 1999; Lacombe et al., 2000), or K^+ inward (KAT1: Ichida et al., 1997; Szyroki et al., 2001; KAT2: Pilot et al., 2001) and outward (GORK: Ache et al., 2000) fluxes in guard cells, leading to stomatal opening/closing.

To adapt to fluctuating K^+ availability in the environment and to cope with other stresses, plants need to tightly regulate K^+ transport at both the whole plant and the cell level (Kochian and Lucas, 1988; Schroeder et al., 1994). Studies aimed at revealing the molecular determinants of these regulations have highlighted mechanisms likely to target Shaker K^+ channels at both the transcriptional and post-translational levels. Expression studies have revealed that transcript levels of Shaker channels are sensitive to hormones (Gaymard et al., 1998; Philippar et al., 1999; Lacombe et al., 2000), sugar synthesis and accumulation, and environmental signals (Deeken et al., 2000). At the post-translational level, indications have been found for regulation by ATP and cyclic GMP (Hoshi, 1995), phosphorylation events (Li et al., 1994; Armstrong et al., 1995; Tang and Hoshi, 1999), functional interactions with the cytoskeleton (Hwang et al., 1997), 14-3-3 proteins (Saalbach et al., 1997; Booij et al., 1999), sulfonylurea receptors (Leonhardt et al., 1997), syntaxins (Leyman et al., 1999), and G proteins (Wu and Assmann, 1994; Wang et al., 2001).

Searches for interacting proteins have been focused on the KAT1 guard cell channel, which has been shown to be phosphorylated by calcium-dependent and abscisic acid (ABA)–regulated protein kinase activities (Li et al., 1998; Mori et al., 2000). A homolog of animal Shaker channel β-subunits has been identified in the Arabidopsis genome and shown to interact physically with KAT1 (Tang et al., 1996). This channel partner protein, named KAB1, has been suggested to stabilize KAT1 in the membrane (Zhang et al., 1999). No other couple channel-interacting protein has been identified at the molecular level to date. In the work reported here, our aim was to identify regulating partners of the AKT2 channel, which displays a very broad expression pattern (Lacombe et al., 2000), suggesting tissue-specific regulation mechanisms, and a gating mode, which has been suggested to be regulated post-translationally (Dreyer et al., 2001).

[1] To whom correspondence should be addressed. E-mail cherel@ensam.inra.fr; fax 33-499-612-930.

Article, publication date, and citation information can be found at www.plantcell.org/cgi/doi/10.1105/tpc.000943.

The *AKT2* gene was isolated initially (Cao et al., 1995) as a homolog of *KAT1*. In situ hybridization allowed the localization of *AKT2* expression in phloem tissues of aerial parts (Marten et al., 1999). Use of the more sensitive technique of promoter-driven expression of the *Escherichia coli* β-glucuronidase (*GUS*) reporter gene revealed *AKT2* promoter activity mainly in the phloem of all plant organs but also, at a lower level, in other cell types of the leaf blade, such as mesophyll, epidermis, and guard cells (Lacombe et al., 2000). The presence of low levels of *AKT2* mRNA in guard cells has been confirmed by reverse transcriptase–mediated polymerase chain reaction (RT-PCR) experiments (Szyroki et al., 2001). Recently, electrophysiological characterization of *akt2* knockout mutant plants has provided definitive evidence that AKT2 is expressed and functional in the mesophyll plasma membrane (Dennison et al., 2001).

AKT2 displays unique functional features among Shaker channels, being the only member of this family able to mediate both K^+ influx and efflux. Characterized in heterologous systems, it behaves as a weakly inwardly rectifying channel, displaying both time-dependent hyperpolarization-activated and instantaneous leak-like current components (Marten et al., 1999; Lacombe et al., 2000). These two kinetic components of the total AKT2 current correspond to two subpopulations of AKT2 channels that display distinct gating modes (Dreyer et al., 2001). It has been demonstrated that a given channel can switch from one gating mode to the other. The mechanisms that trigger these transitions have not been identified, but phosphorylation/dephosphorylation events have been suggested (Dreyer et al., 2001). In this context, it is interesting that AKT2 was isolated recently as a putative partner of a plant protein phosphatase involved in ABA signaling, AtPP2CA, on the basis of two-hybrid system screening with this phosphatase as the bait (Vranova et al., 2001). No additional experiments were reported to confirm the interaction or to assess its functional significance in plants.

Using AKT2 as the bait for two-hybrid system screening, we found a positive cDNA encoding a large C-terminal fragment of AtPP2CA. Here, we provide biochemical and functional evidence that AtPP2CA interacts with AKT2, at least in heterologous systems, and that AKT2 and AtPP2CA have largely overlapping expression patterns. Unique functional effects on the channel activity are presented, and their possible physiological meanings are discussed.

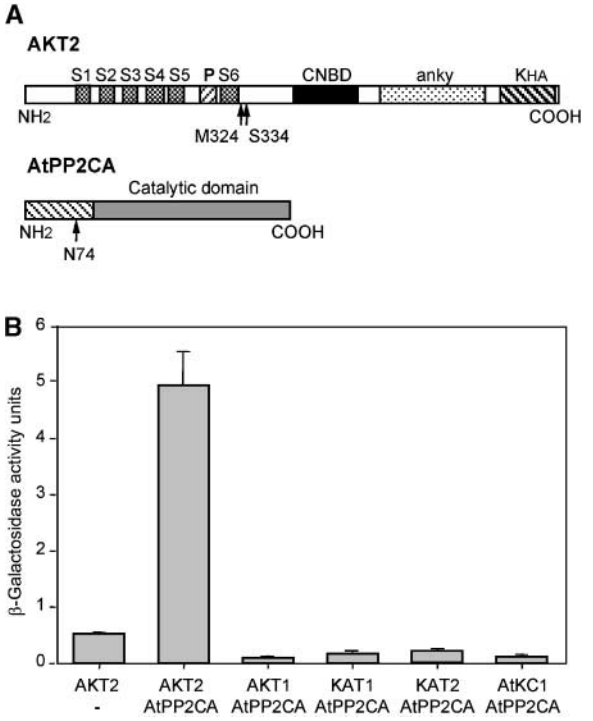

Figure 1. Two-Hybrid Interaction of AtPP2CA with Potassium Channels of the Shaker Family.

(A) Scheme of the structural domains of AtPP2CA protein phosphatase and the AKT2 K^+ channel. The positions of the first amino acids of AKT2 regions used as baits (Ser-334 for the construct used for two-hybrid screening and Met-324 [beginning of the intracytoplasmic C terminus] for the construct used in subsequent two-hybrid experiments) and of the first amino acid of the AtPP2CA C-terminal region obtained after two-hybrid screening (Asn-74) are indicated. In AtPP2CA, the hatched area represents the N-terminal domain, which is not conserved within the PP2C family. S1 to S6 indicate the six transmembrane segments of the channel hydrophobic core, with a pore-forming domain (P) present between S5 and S6. anky, ankyrin domain; CNBD, putative cyclic nucleotide binding domain; KHA, domain rich in acidic and hydrophobic amino acids, characteristic of plant channels of the Shaker family.

(B) Two-hybrid interaction tests between AtPP2CA and other channels. The AtPP2CA catalytic domain (from Asn-74, cDNA fragment in pGAD10 vector) was tested against the intracytoplasmic C-terminal domains (downstream of the S6 last transmembrane segment, cDNA inserts in pGBT9 vector) of Shaker potassium channels. β-Galactosidase activities, measured for 1-mL culture pellets with *o*-nitrophenyl β-D-galactopyranoside as a substrate, are expressed as OD_{420} per min × $1000/OD_{600}$ of the culture medium. The left bar shows AKT2 (from Met-324) tested with the free Gal4 activator domain (using the empty pGAD10 vector).

RESULTS

Two-Hybrid Interactions in Yeast

With a large AKT2 C-terminal region as the bait (from Ser-334 to the last amino acid of the channel, Ile-802) (Figure 1A), screening of the Arabidopsis cDNA library (see Methods) resulted in the isolation of numerous positive cDNA clones. Cross-hybridization studies and sequence analyses allowed us to identify nine groups of overlapping cDNA fragments, each forming a pool of truncated copies of the same mRNA. Among the cDNA groups for which high signals were obtained in two-hybrid tests, one corresponded to KAT1, a Shaker channel already shown to interact with AKT2 in functional tests (Baizabal-Aguirre et al., 1999),

and another corresponded to AtPP2CA (Kuromori and Yamamoto, 1994), which is a member of the protein phosphatase 2C (PP2C) family (Rodriguez, 1998). Plant PP2Cs display two structural domains: an N-terminal variable domain, and a conserved catalytic domain (Rodriguez, 1998). Only the sequence (from amino acid 74) (Figure 1A) encoding the catalytic domain was present in the *AtPP2CA* clones identified during the two-hybrid screening.

We further checked the specificity of the AKT2–AtPP2CA interaction by testing the C-terminal domains of five different Arabidopsis Shaker channels (including AKT2) with the AtPP2CA construct. Hybrid constructs encoding the C-terminal region (the whole cytoplasmic domain downstream of the S6 segment) of AKT2 (from Met-324; see Methods), AKT1 (from His-294; Daram et al., 1997), KAT1 (from Thr-303; Urbach et al., 2000), KAT2 (from Arg-316; Pilot et al., 2001), or AtKC1 (from His-330) were used. With the AtPP2CA catalytic domain fused to the Gal4 activator domain, none of the DNA binding domain constructs except the one corresponding to AKT2 gave a positive signal (Figure 1B). The reciprocal tests with AtPP2CA as the bait (fused to the Gal4 DNA binding domain) were performed and revealed much higher background levels, compared with the previous two-hybrid configuration, as a result of artifactual activation of the reporter gene by the AtPP2CA hybrid polypeptide. However, a signal of higher than background level was observed with the AKT2 C-terminal region (data not shown). It should be noted that all of the two-hybrid constructs used in these experiments had been validated previously by the observation of positive results in interaction tests with channel C-terminal regions, either identical to the bait or different (Daram et al., 1997; Urbach et al., 2000; Pilot et al., 2001; I. Chérel, unpublished results), plant potassium channels being multimeric proteins.

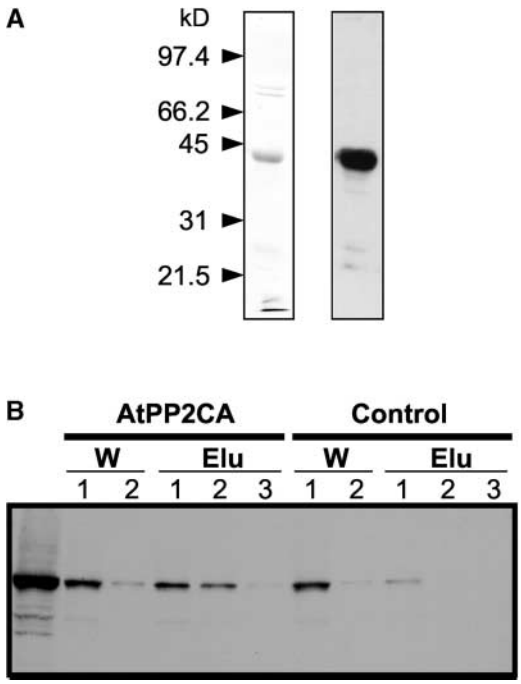

Figure 2. AKT2-CT Binding on Nickel-Affinity Agarose Beads Loaded with His-Tagged AtPP2CA Fusion Polypeptide.

(A) His-tagged AtPP2CA binding on the metal affinity column. The Ni-NTA matrix was mixed with an extract from bacteria expressing the His-tagged AtPP2CA polypeptide, washed, and treated with 250 mM imidazole to elute the nickel from the matrix with proteins associated to it. The eluate was analyzed by SDS-PAGE. At left is a Coomassie blue–stained gel, and at right is a protein gel blot revealed with a monoclonal antibody directed against the tetrahistidine peptide (Qiagen).

(B) Biochemical evidence for interaction between AtPP2CA and AKT2. The *Sf*9 cell extract containing AKT2-CT (first lane) was loaded either onto the AtPP2CA column (harboring AtPP2CA bound by its hexahistidine tag) or onto an empty control Ni-NTA column. Columns were washed twice (fractions W 1 and W 2), and proteins were eluted with 250 mM imidazole (three successive elutions: fractions Elu 1, Elu 2, and Elu 3). Every well was loaded with a 30-μL sample.

AKT2 Is Retained on AtPP2CA-Coated Gel Beads

Experiments were performed with the AtPP2CA C-terminal polypeptide (from Asn-74) tagged with a hexahistidine peptide (His tag) at its N terminus. Small affinity columns (each containing 150 μL of agarose beads) were prepared with nickel–nitrilotriacetic acid agarose (Ni-NTA) matrix. In a first step, the binding of His-tagged AtPP2CA produced in *E. coli* to the Ni-NTA matrix was checked by incubating the matrix with the *E. coli* extract, washing, and directly eluting with 250 mM imidazole to release proteins bound to nickel. The most abundant polypeptide eluted from the gel had an apparent molecular mass of ~42 to 43 kD. This band was identified as the His-tagged polypeptide (predicted molecular mass of 40 kD) by protein gel blot analysis with an antibody raised against tetra-histidine peptide (Figure 2A). This result indicates that the AtPP2CA His-tagged protein represented the major polypeptide retained on the matrix, contaminants being present as traces only.

In a second step, another column coated with His-tagged AtPP2CA (AtPP2CA column) and washed as described above but without the elution step was used to test the binding of the AKT2 C-terminal polypeptide (from Met-324, hereafter referred to as AKT2-CT). Because nontagged proteins can interact with the Ni-NTA matrix, especially when the purification is performed under native conditions, a control 150-μL column, for which the AtPP2CA binding step was omitted, was treated exactly like the AtPP2CA column. Each column (with or without bound AtPP2CA) was loaded with an extract from *Sf*9 cells (3.5 mg of protein) expressing AKT2-CT, washed under mild conditions, and treated with 250 mM imidazole. Fractions collected at different steps of the purification procedure were analyzed by SDS-PAGE. AKT2-CT was not detectable after Coomassie blue staining

of the acrylamide gel, and silver staining did not allow its identification with certainty. However, protein gel blot analysis performed with anti-AKT2 serum revealed a polypeptide (Figure 2B) with an apparent molecular mass (58 kD) higher than the theoretical molecular mass of the AKT2-CT polypeptide (54 kD) but corresponding exactly to that of the band that appeared specifically in extracts from AKT2-CT–expressing *Sf*9 cells (E. Michard, unpublished results).

The 58-kD band was detected at a relatively high level in the first wash from both columns (Figure 2B, lanes W 1) but was barely detectable in the second wash (Figure 2B, lanes W 2). After elution with imidazole, a significant amount of AKT2-CT was recovered from the AtPP2CA column in the first two elution fractions (Figure 2B, AtPP2CA column, lanes Elu 1 and Elu 2). On the other hand, the protein gel blot corresponding to the control column revealed only a faint band, probably resulting from nonspecific binding to free sites of the matrix, and present solely in the lane corresponding to the first elution fraction (Figure 2B, control column, lane Elu l). Similar results were obtained in a subsequent experiment comparing the AtPP2CA column with another control column that was loaded previously with an extract from bacteria that were able to synthesize only the His tag (transformed with the empty vector; data not shown). Thus, all of the data indicated that AtPP2CA and AKT2 interact.

AtPP2CA Gene Expression Overlaps That of *AKT2* and Is Upregulated by ABA in Shoots and Roots

Four-week-old plants harboring the *AtPP2CA* promoter (the 3-kb region upstream from the initiator ATG) fused to the *GUS* reporter gene and grown in a greenhouse were tested for GUS activity. Six independent transformants were examined. Blue staining (revealing GUS activity) was detected in several organs of the plant in both roots and aerial parts (Figure 3). In the root system, the staining was faint and present mainly in the stele (Figure 3A). In aerial parts, staining was much more intense and was found in photosynthetic and reproductive organs. It was concentrated in the veins of cotyledons and leaves (Figures 3B and 3C), essentially at the periphery and at the tip in the case of mature leaves of the rosette and caulinary leaves. Staining also was visible in mesophyll cells between stained veins and in hydathodes, which are structures involved in the process of guttation (Figure 3C). GUS activity also was detected in guard cells (Figures 3F and 3G). In reproductive organs, intense staining was present in the pollen (Figure 3D) and in the receptacle below the green siliques (Figure 3E). Cross-sections of roots and leaves revealed that in the vascular system, GUS activity was detected only in phloem tissues (Figures 3H and 3I).

The possibility of coexpression of the *AKT2* and *AtPP2CA* genes in the same cell type was tested further by RT-PCR. Mesophyll cells are easy to isolate, and AKT2 channels ac-

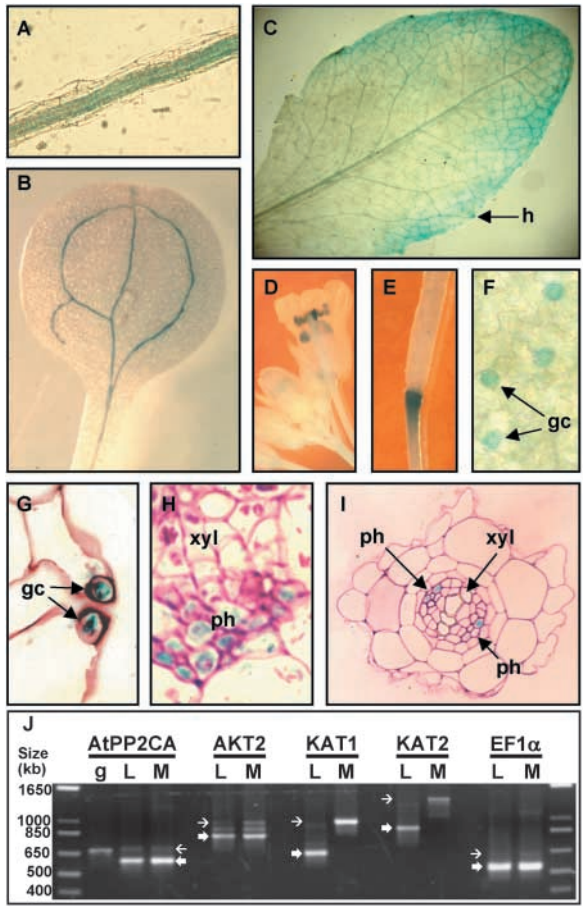

Figure 3. Expression Pattern of the *AtPP2CA* Gene Overlaps That of the *AKT2* Gene.

(A) to **(I)** Localization of *AtPP2CA* promoter activity in Arabidopsis transgenic plants grown on compost in the greenhouse.
(A) Young lateral root.
(B) Cotyledon leaf.
(C) Mature leaf.
(D) Flowers.
(E) Green silique.
(F) Mature leaf (enlargement showing guard cells).
(G) Cross-section of a stomatal chamber.
(H) Vascular area of a petiole.
(I) Root cross-section.
gc, guard cells; h, hydathode; ph, phloem; xyl, xylem.
(J) RT-PCR experiments performed on total RNA isolated from whole leaves (L) or mesophyll protoplasts (M). Thin arrows indicate the expected size of the genomic DNA fragments amplified with the pairs of primers used in the test, and thick arrows indicate that of the cDNA fragments. These sizes are in kilobases (cDNA/genomic): 600/685 for *AtPP2CA*, 823/993 for *AKT2*, 654/987 for *KAT1*, 896/1301 for *KAT2*, and 546/639 for *EF1α*. g indicates an amplification of genomic DNA with the *AtPP2CA* primers.

count for half of their K^+ permeability (Dennison et al., 2001). RT-PCR experiments were performed with total RNA isolated from mesophyll cells and whole leaves from the same plants (Figure 3J). As negative controls, we used two other Shaker channel genes: *KAT1*, which is expressed in guard cells (Nakamura et al., 1995), and *KAT2*, which is expressed in guard cells and minor veins (Pilot et al., 2001). The transcripts of these genes were detected in whole leaves but not in mesophyll cells, for which only genomic DNA present as a contaminant in our RNA preparation could be amplified. On the contrary, *AtPP2CA* and *AKT2* transcripts were detected in mesophyll cells (Figure 3J). Other primer pairs (two for *AKT2* and one for *KAT1* and *KAT2*) led to similar results (data not shown).

Twelve independent experiments with transgenic plants transformed with the *GUS* reporter gene construct and grown in the greenhouse revealed reproducible expression patterns but with a high variability in GUS staining intensity. The entire set of observations led us to the hypothesis that *AtPP2CA* promoter activity was affected by unidentified changes in environmental conditions. In this context, we studied the effects of ABA on the expression of the *GUS* construct. Plants grown in the greenhouse but carefully watered to avoid any drought stress were transferred either onto a control $CaSO_4$ solution or onto the same solution supplemented with 100 μM ABA. Whereas no GUS activity was detected in the former plants, strong GUS staining was observed in the latter plants after a 3-hr ABA treatment. The induction by ABA was especially visible in leaf veins and in the root stele (Figure 4A).

After longer ABA treatments (6 to 24 hr), roots and leaves were stained uniformly (data not shown). Consistent with these observations, RNA gel blot analyses revealed a strong induction of *AtPP2CA* gene expression upon ABA treatment (Figure 4B) in shoots (in agreement with the RNA gel blot data presented by Tähtiharju and Palva [2001]) but also in roots (two independent experiments). The transcript distribution between shoots and roots was largely in favor of roots in this case, whereas the opposite situation was observed with untreated plants grown in the greenhouse. This kind of inversion is similar to that reported for other ABA-induced genes when a physiological situation (drought stress) is compared with an ABA treatment applied to the root system (Gosti et al., 1995).

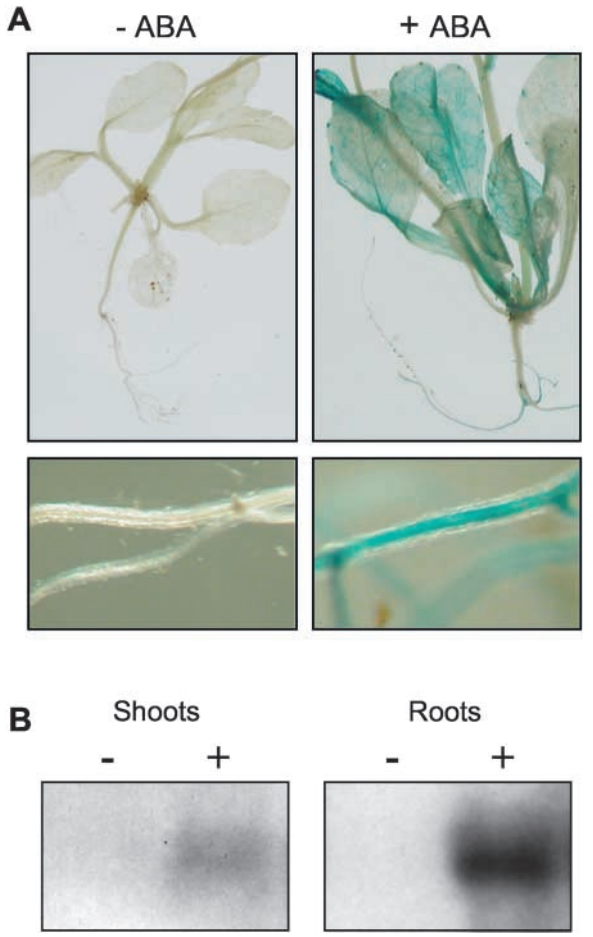

Figure 4. Induction of AtPP2CA Expression by ABA.

(A) AtPP2CA promoter activity (GUS reporter gene expression) in 3-week-old plantlets from the same transgenic line grown in the greenhouse and transferred for 3 hr to 250 μm $CaSO_4$ (left) or 250 μm $CaSO_4$ + 100 μm ABA (right). Top, whole plantlets; bottom, roots.

(B) RNA gel blot analysis performed on 3-week-old plantlets grown hydroponically in magenta boxes and transferred to control medium (−) or treated for 3 hr with 100 μm ABA (+).

AtPP2CA Inhibits the AKT2 Current in COS Cells

The functional effects of the AtPP2CA–AKT2 interaction were sought by patch clamping transfected COS cells (see Methods). The currents recorded in cells expressing AKT2 alone were approximately three times larger than those in cells coexpressing AKT2 and AtPP2CA (Figure 5A, middle and bottom, respectively). To ascertain the specificity of the inhibitory effect of AtPP2CA on AKT2 current, a control experiment was performed by coexpressing AtPP2CA with another Arabidopsis Shaker channel, KAT1. In accordance with the fact that this plant potassium channel did not interact with AtPP2CA in the two-hybrid system, KAT1 currents were not affected by the presence of AtPP2CA in COS cells (Figure 5B).

As described previously (Lacombe et al., 2000), the AKT2 macroscopic current showed an instantaneous nonrectifying (leak-like) component, which superimposed on a time-dependent hyperpolarization-activated component (Figure 5A). The inhibitory effects of AtPP2CA on these two components were quantified, revealing a larger decrease of the instantaneous leak-like current. For instance, in the experiment

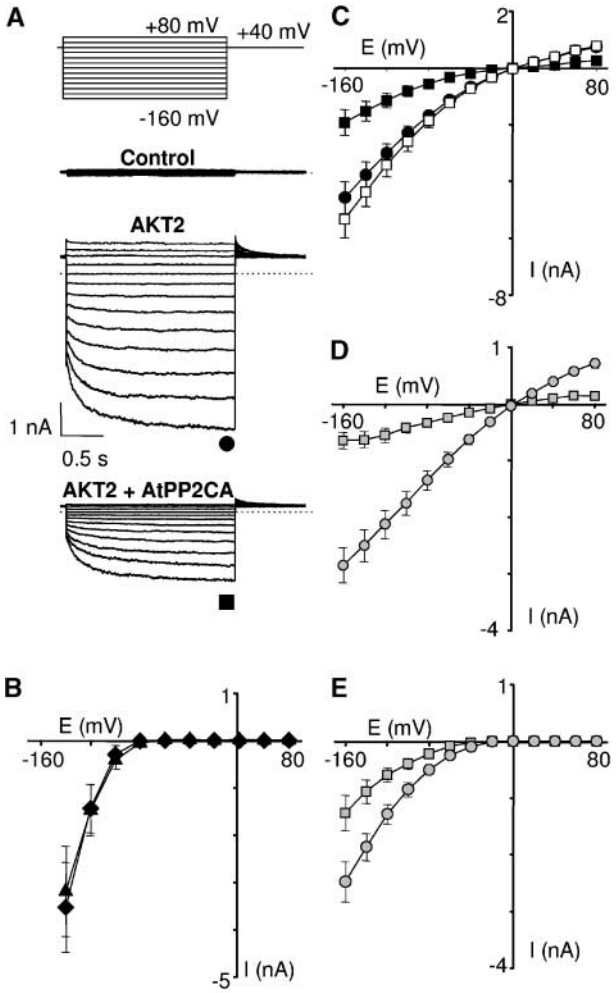

Figure 5. Modulation of AKT2 Currents by Coexpression with AtPP2CA in COS Cells.

(A) Typical current traces evoked by the voltage protocol indicated at top in COS cells transfected with pIRES alone (control) or cotransfected with pIRES and pCI-AKT2 (AKT2) or pIRES-AtPP2CA and pCI-AKT2 (AKT2 + AtPP2CA) at 3 days after transfection.

(B) Current-voltage relationship for KAT1 expressed alone (diamonds) or together with AtPP2CA (triangles).

(C) Current-voltage curves recorded in a batch of COS cells cotransfected with pCI-AKT2 and pIRES (open squares), pIRES-AtPP2CA (closed squares), or pIRES-AtPP2CA* (null mutation; closed circles [note that closed circles are hidden by the open squares at positive potential values]). Cs^+ controls (data not shown) were used to ensure that currents were generated by potassium-selective channels. Data are means ±SE, with $n > 6$ in each case.

(D) and **(E)** Instantaneous **(D)** and time-dependent **(E)** currents taken from data presented in Figure 3C for COS cells cotransfected with pIRES-AtPP2CA and pCI-AKT2 (squares) or pIRES and pCI-AKT2 (circles).

reported in Figure 5C, the inhibition of AKT2 current (2.8-fold) was attributable to a 4.5-fold decrease in the instantaneous leak-like component and a 2-fold decrease in the hyperpolarization-activated component (Figures 5D and 5E, respectively; inhibition computed at −160 mV). As a result, the AKT2 current was not only decreased in magnitude but also changed qualitatively. A so-called "leak index" was defined for the AKT2 current to appreciate the qualitative changes.

In the experiments described above (Figure 5), where the equilibrium potential for K^+ (E_K) was 0 mV, an "ideal" K^+-selective leak conductance (devoid of rectification) should result in a linear current-voltage (I-E) curve crossing the origin of the graph. With such a conductance, the amount of current recorded at −160 mV ($|I_{-160}|$) would be four times that recorded at +40 mV ($4 \cdot I_{+40}/|I_{-160}| = 1$). Conversely, a perfect K^+-selective hyperpolarization-activated channel should display a flat I-E curve for voltages above the activation potential with no outward current ($4 \cdot I_{+40}/|I_{-160}| = 0$). The ($4 \cdot I_{+40}/|I_{-160}|$) ratio was defined as the AKT2 leak index. Data shown in Figure 5C yielded leak indexes of 0.39 ± 0.06 ($n = 6$) for AKT2 expressed alone and 0.20 ± 0.04 ($n = 8$) for AKT2 coexpressed with AtPP2CA, highlighting the fact that the functional interaction between AtPP2CA and AKT2 resulted in a significant decrease in the leak-like current.

The requirement of protein phosphatase activity for the observation of the AtPP2CA effect on AKT2 was checked by introducing a null mutation in the catalytic site of the enzyme. The G139D mutation is known to result in the complete loss of PP2C activity (Sheen, 1998). When coexpressed with AKT2 in COS cells, the null G139D mutant protein poorly modified the AKT2 currents (Figure 5C, closed circles).

Coexpression in *Xenopus laevis* Oocytes Further Confirms the Functional Interaction between AtPP2CA and AKT2

In a first set of experiments, comparison of AKT2 currents in oocytes expressing AKT2 alone or coexpressing AKT2 and AtPP2CA provided further evidence that AtPP2CA inhibits AKT2 activity (current reduced to 40% of the control value; $n = 6$; data not shown). Detailed analyses revealed that the functional interaction also resulted in qualitative changes in AKT2 current, as in COS cells, the leak-like component being more affected than the hyperpolarization-activated component. Indeed, when calculated as described above, the leak index was found to be 0.40 ± 0.02 ($n = 6$) for AKT2 coexpressed with AtPP2CA and 0.52 ± 0.07 ($n = 6$) for AKT2 expressed alone (Figures 6B and 6D, closed symbols).

In a second set of experiments, the effects of AtPP2CA on AKT2 current were investigated in the presence or absence of vanadate, a permeant nonspecific phosphatase inhibitor classically used for this kind of approach in *Xenopus laevis* oocytes (McNicholas et al., 1994; Becq et al., 1997; Tsai et al., 1999). It was verified that vanadate bath solution per-

fused for 1.5 hr before the current recordings had no effect on the membrane conductance of water-injected oocytes (Figure 6A). In oocytes expressing AKT2 alone, the vanadate treatment induced a slight increase (~20%) in the AKT2 current (Figure 6B). A much larger increase was observed in oocytes coexpressing AKT2 and AtPP2CA (Figures 6C and 6D). Figure 6C shows current recordings obtained in an oocyte expressing both the K^+ channel and the protein phosphatase before (top) and after (bottom) vanadate treatment. The corresponding I-E curve shown in Figure 6D indicates that the treatment resulted in a strong increase (~2.5 times) of the AKT2 current.

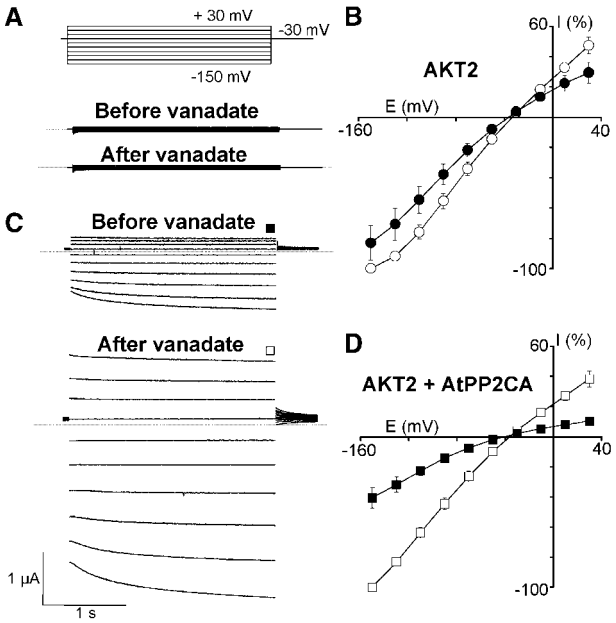

Figure 6. Coexpression of AKT2 and AtPP2CA in Xenopus Oocytes.

(A) Control experiment performed with water-injected oocytes before and after a 1.5-hr treatment with 3 mM vanadate.

(B) Current-voltage (I-E) curves for oocytes injected with pCI-AKT2 alone before (closed symbols) and after (open symbols) vanadate treatment. Mean values and standard errors for at least five independent measurements (oocytes) are shown ($n > 5$). Data were normalized to the current value at −150 mV in the presence of vanadate (100%). The average of this reference value was −1.78 µA. Cs^+ control recordings performed before and after vanadate treatment (data not shown) indicated that the currents were generated by potassium-selective channels.

(C) Typical currents recorded in oocytes coinjected with pCI-AtPP2CA and pCI-AKT2 (ratio of 2:1) before and after vanadate treatment.

(D) Current-voltage (I-E) curves for oocytes coinjected with pCI-AtPP2CA and pCI-AKT2 before (closed symbols) and after (open symbols) vanadate treatment. Values shown and data normalization were as in **(B)**. The average reference value (100%) was −2.18 µA.

The leak index was shifted from 0.40 ± 0.02 before vanadate treatment to 0.60 ± 0.08 ($n = 5$) after the treatment, indicating that inhibition of phosphatase activity by vanadate favored the leak-like component. Cs^+ controls (see Methods) were used to ascertain that neither an endogenous current nor a nonspecific leak had appeared during the 1.5-hr vanadate treatment (data not shown). Thus, the combined data indicate both that the endogenous oocyte phosphatases affected AKT2 activity much less than AtPP2CA and that the AKT2 inhibition by AtPP2CA was counteracted by the use of a phosphatase inhibitor. In conclusion, modulations of AKT2 current intensity and rectification by AtPP2CA are observed regardless of the heterologous system, Xenopus oocytes or mammalian cells, and are caused by the phosphatase activity of AtPP2CA.

DISCUSSION

Physical and Functional Interactions of AtPP2CA with AKT2

Using the yeast two-hybrid system, we isolated AtPP2CA as a putative AKT2-interacting protein. The two-hybrid system allows a rapid screen for putative partners of a given protein. However, the isolation of a positive clone with this technique cannot be taken as proof of interaction because of the abundance of artifactual responses. The reciprocal test, with the putative partner fused to the Gal4 DNA binding domain and the target protein fused to the Gal4 activator domain, eliminates many false-positive results. A positive response in both test configurations is taken as a strong indication of true physical association (Allen et al., 1995).

In the case of the AKT2–AtPP2CA interaction, in spite of a high background signal, we confirmed the two-hybrid interaction in the reciprocal test, in agreement with the recent isolation of AKT2 by screening of a two-hybrid cDNA library using AtPP2CA as the bait (Vranova et al., 2001). In the same report, it was indicated that a deletion of the last 180 amino acids of the AtPP2CA catalytic domain abolished the two-hybrid interaction, revealing that this region either contains the binding site for AKT2 or is necessary for the stability and/or proper folding of the AtPP2CA polypeptide. The AtPP2CA clone that was isolated during our two-hybrid screen essentially encodes the AtPP2CA C-terminal (catalytic) domain, providing evidence that this domain (Figure 1) is involved directly in the interaction with AKT2.

Direct physical interaction between AKT2 and AtPP2CA was further confirmed by the demonstration of in vitro binding of AKT2-CT onto a Ni-NTA agarose column coated with AtPP2CA. The binding affinity between a protein phosphatase and its substrate is expected to be low. Indeed, a large proportion of AKT2-CT flowed through the AtPP2CA-coated column. However, compared with the control columns, which retained only trace amounts of AKT2-CT (nonspecific

binding), the AtPP2CA column bound a significant amount of channel polypeptide (Figure 2). Thus, the hypothesis that AtPP2CA can interact physically with AKT2 is supported by results from two independent approaches, two-hybrid tests and in vitro binding assays. Such an interaction involving a PP2C and a channel has been observed between the human PP2Cα and the cystic fibrosis transmembrane regulator anion channel (Travis et al., 1997).

Coexpression of AKT2 and AtPP2CA in COS cells and Xenopus oocytes revealed a modulation of AKT2 channel activity that likely results from the physical association of the two proteins. Dephosphorylation events mediate this functional interaction, because the changes in channel activity are sensitive to vanadate and suppressed by a point mutation in the catalytic site of the AtPP2CA protein, resulting in the loss of its phosphatase activity. Thus, all of the data support the hypothesis that AtPP2CA can bind to and dephosphorylate AKT2, leading to changes in K^+ current features. It should be noted that these changes are quantitative and qualitative, with a decrease in both current amplitude and leaky behavior. Conversion of a potassium leak channel into a voltage-dependent channel induced by changes in phosphorylation status was described in animal cells recently, but in an opposite way, with phosphorylation events leading to increased rectification: the addition of ATP and commercially available protein kinase A was found to decrease the activity of the hippocampal K^+ channel KCNK2 and to convert this protein from a voltage-insensitive open pore into a voltage-dependent outward rectifier (Bockenhauer et al., 2001). AKT2 is a channel displaying such an interconversion for which a specific regulatory partner responsible for this behavior has been identified.

Possible Links to Other ABA-Induced Phosphatase Activities

AtPP2CA is one of the closest relatives of ABI1 and ABI2, two PP2Cs known to be involved in ABA hormone signaling (Leung and Giraudat, 1998; Rodriguez, 1998). Under drought stress conditions, ABA mediates stomatal closure, allowing limitation of water loss (reviewed by Blatt, 2000). *ABI1* and *ABI2* genes are involved in most aspects of ABA response (Leung et al., 1997). Genetic studies have established that ABI1 and ABI2 are negative regulators of ABA transduction signals (Gosti et al., 1999; Merlot et al., 2001). The concomitant increases of *ABI1* and *ABI2* mRNA levels and corresponding protein phosphatase activities induced by ABA have led to a model (Merlot et al., 2001) in which ABI1 and ABI2 take part in a negative feedback regulatory loop that continuously resets the ABA signaling cascade to adjust the response to the ABA level.

AtPP2CA overexpression results in the inactivation of an ABA-responsive promoter (Sheen, 1998), and the encoded protein plays a role during cold acclimation by counteracting ABA effects (Tähtiharju and Palva, 2001). The inhibitory effect of AtPP2CA on the AKT2 channel also may counteract the ABA-induced increase in AKT2 expression (Lacombe et al., 2000). Like that of *ABI1* and *ABI2*, the *AtPP2CA* mRNA is induced by ABA. Together, these results suggest that the general function of AtPP2CA could be similar to that of ABI1 and ABI2, namely, to mediate a negative control of ABA signaling in response to an increase in the hormone level. Because of the pleiotropic effects of these plant PP2Cs, it is likely that several substrates may be recognized as targets. Ion channels have been proposed to be regulated by direct or indirect interactions with PP2Cs. For example, overexpression of a mutant ABI1 protein in tobacco results in the deregulation of anion channels (Pei et al., 1997) and of voltage-gated inward and outward K^+ rectifiers in guard cells (Armstrong et al., 1995). No substrate protein of either ABI1 or ABI2, however, has been identified to date.

Because the interaction between AKT2 and AtPP2CA involves the well-conserved catalytic C-terminal domain of AtPP2CA, the possibility exists for an interaction between AKT2 and other closely related PP2Cs. These are ABI1 (48% identity with AtPP2CA within the catalytic domain), ABI2 (46%), AtPP2C-HA (44%) (Rodriguez, 1998), and others that are most similar to AtPP2CA (60 to 66% identity). Although ABI1 was not found to react with AKT2 in a two-hybrid assay (Vranova et al., 2001), this question is worth investigating.

Physiological Meaning of AKT2 Regulation by AtPP2CA

Under physiological conditions, the expression of both *AKT2* and *AtPP2CA* was observed mainly in shoots. Detailed comparison of the GUS data reveals that the expression pattern of *AtPP2CA* (Figure 3) clearly overlaps that of *AKT2* (Marten et al., 1999; Lacombe et al., 2000), especially in the phloem vasculature and the receptacle below the siliques, tissues that constitute the main zones of expression of the two genes. *AtPP2CA* also is expressed in leaf mesophyll and guard cells (Figure 3), where low levels of *AKT2* promoter activity (Lacombe et al., 2000) and of *AKT2* transcripts (Szyroki et al., 2001) (Figure 3J) have been detected. Thus, the AtPP2CA phosphatase can be expected to regulate AKT2 current amplitude and rectification in several cell types. Also supporting this hypothesis, the electrophysiological properties of AKT2 are similar to those of a K^+ channel detected in mesophyll cells, PKC1 (Spalding and Goldsmith, 1993), which seems to be activated by phosphorylation.

In the phloem vasculature, where AKT2 and AtPP2CA display their highest expression levels, AKT2 could allow both K^+ loading or unloading, as proposed by Lacombe et al. (2000). High ABA levels have been found in phloem tissues, and the hormone accumulation is enhanced during water stress (Sotta et al., 1985). ABA has been proposed to pro-

mote phloem unloading of Suc, possibly by inactivating the proton pump (reviewed by Delrot and Bonnemain, 1985). Under such conditions, AKT2 might contribute to potassium release. Upregulation of *AtPP2CA* expression by ABA (Figure 4), resulting in the inhibition of AKT2 channels and the switch to the rectifying gating mode, would control this release and thereby play a role in the control of membrane polarization (see below) and Suc transport. Also, AKT2 activity and its regulation by AtPP2CA might modify the K^+ gradient in the phloem vasculature between sources and sinks, which has been hypothesized to play a major role in steepening the gradient of hydrostatic pressure driving the phloem sap toward the sinks (Vreugdenhil, 1985).

With respect to this hypothesis, it is worth noting that concomitant sharp decreases in phloem sap flow rate and phloem K^+ content can be evoked by stresses such as repeated cold shocks (Fromm and Bauer, 1994). Finally, it was reported recently that the *AKT2* gene and an *AKT2*-like gene of *Vicia faba*, *VFK1*, are regulated by light in the phloem. Both *AKT2* and *VFK1* transcripts are induced by light and products of CO_2 assimilation (Deeken et al., 2000; Ache et al., 2001), and the depolarization evoked by Fru through *Vicia* phloem cells is K^+ dependent (Ache et al., 2001). Thus, studying the possible response of AtPP2CA activity to light and photosynthesis should result in a more global understanding of the role of the AKT2–AtPP2CA interaction in planta.

At the cell level, the AKT2–AtPP2CA interaction would allow the regulation of membrane potential, as discussed below. In plant cells, two kinds of K^+ channels, activated either by membrane hyperpolarization or membrane depolarization, dominate membrane conductance (Blatt, 1992; Maathuis and Sanders, 1995). As a result, a voltage range of low conductance is found between the activation threshold of hyperpolarization-activated inwardly rectifying channels and that of depolarization-activated outwardly rectifying channels. Compared with the other K^+ channels identified to date at the molecular level, AKT2 is unique in its ability to be open in the entire physiological voltage range (Figures 6B and 6D). Thus, in the low-conductance voltage range, changes in AKT2 activity, involving functional interaction with AtPP2CA, could markedly affect the membrane permeability to K^+ and thereby play a role in the control of cell membrane potential.

For instance, in combination with a decrease in the activity of the electrogenic H^+-ATPase, AKT2 activity could enable controlled membrane depolarization in a voltage range within which strictly voltage-gated K^+ channels are inactive. The AtPP2CA phosphatase then could control the ABA-induced membrane depolarization that has been observed in some cell types (guard cells: Thiel et al., 1992; mesophyll cells: Felle et al., 2000) by inhibiting AKT2 current. AKT2 and the AtPP2CA phosphatase could thereby play a role similar to the one fulfilled in animal cells by "background" leak K^+ channels (Lesage and Lazdunski, 2000) and their phosphatase/kinase partners (not yet identified; Bockenhauer et al., 2001) in the control of cell membrane potential. Poorly rectifying instantaneous currents often are neglected in whole cell recording and simply subtracted, being considered nonselective or even artifactual currents. Our data clearly indicate that a leak current, controlled by phosphorylation/dephosphorylation events and likely to have major physiological importance, does exist in plant cells.

In conclusion, AtPP2CA can interact physically and functionally with AKT2, regulating the activity and unique gating features of this channel. The expression patterns of the two genes are very similar, not only with respect to tissue specificity but also regarding regulation by ABA. Therefore, the functional interaction of AKT2 and AtPP2CA, under ABA control, could play a role in the regulation of membrane conductance to K^+ and membrane potential as well as in related functions at the whole plant level such as phloem transport.

METHODS

Two-Hybrid Constructs

An *AKT2* cDNA encoding a long C-terminal fragment (from amino acid 334 to the end of the polypeptide sequence) was obtained from a previous library screening with KAT1 as the bait. This cDNA fragment was fused in frame with the sequence encoding the Gal4 DNA binding domain in plasmid pGBT9 (Bartel and Fields, 1995). The resulting plasmid was used to screen the library. For subsequent tests, a larger fragment (encoding the sequence from amino acid 324) was obtained via NcoI partial digestion and ligated into pGBT9, leading to the creation of the pGBT9-AKT2 plasmid. pGBT9 constructs harboring AKT1, KAT1, and KAT2 sequences encoding channel C-terminal regions were obtained previously (Daram et al., 1997; Urbach et al., 2000; Pilot et al., 2001, respectively). The *AtKC1* fragment (polypeptide sequence from His-330) was obtained by NcoI digestion.

Two-Hybrid cDNA Library Screening and Interaction Tests

Yeast strain Y190 *Saccharomyces cerevisiae* (Bartel and Fields, 1995) was cotransformed with pGBT9 plasmid harboring AKT2 sequence (75 μg) and 15 μg of DNA from a cDNA library designed for two-hybrid screening (Clontech FL4000AB [Palo Alto, CA]) (prepared from 3-week-old green vegetative tissue; 3×10^6 independent transformants), according to Gietz et al. (1992). Transformants were plated on selective medium lacking His, Trp, and Leu (plating medium described by Daram et al. [1997] without His) supplemented with 50 mM 3-aminotriazole. Yeast colonies were replicated on paper sheets (80 g/m^2) and tested for β-galactosidase activity (colony filter assay; Bartel and Fields, 1995). Positive colonies were amplified at 30°C in 2 mL of liquid medium lacking Leu (plating medium [Daram et al., 1997] without agar and supplemented with His and Trp).

After centrifugation, cell pellets were resuspended in 250 μL of 10 mM Tris, 1 mM EDTA, and 200 mM NaCl, pH 8. Two hundred microliters of 0.45-mm glass beads and 250 μL of phenol:chloroform:isoamyl alcohol (25:24:1) were added to each cell suspension, and tubes were vortexed (2×1 min at maximum speed). After a 3-min centrifugation at 15,000*g*, the upper phases were mixed with

500 μL of phenol:chloroform:isoamyl alcohol, vortexed (2 × 1 min), and centrifuged. Aqueous phases were precipitated with 3 volumes of ethanol, and pellets were washed with 70% ethanol and resuspended in 20 μL of water. These DNA preparations were used for plasmid isolation after transformation of *Escherichia coli* and to determine groups of cDNA clones originating from the same mRNA.

For the latter purpose, all cDNA inserts were amplified by polymerase chain reaction (PCR) using oligonucleotides Matchmaker 5′AD and 3′AD (Clontech). Amplification products were mixed with 20 × SSC (one-third volume) (1 × SSC is 0.15 M NaCl and 0.015 M sodium citrate), heat denatured, and spotted onto a nylon membrane (Hybond+). This membrane was hybridized with a ^{32}P-radiolabeled copy of one of the selected cDNAs, which were isolated previously by SalI digestion of the library plasmid and purified twice on an agarose gel. This allowed the identification of clones that hybridized with each cDNA. The membrane then was dehybridized, and the experiment was repeated with another cDNA insert.

For quantitative two-hybrid tests, cells from a 1-mL culture were assayed for reporter gene expression using *o*-nitrophenyl β-D-galactopyranoside as a substrate (Bartel and Fields, 1995).

Generation of a Full-Length *AtPP2CA* cDNA

An internal EcoRI site present in the *AtPP2CA* cDNA sequence was used to generate the full-length cDNA. The original insert from the cDNA library (3′ fragment in pGAD10 vector) was digested with SalI and cloned into pBluescript KS+. A clone displaying the proper orientation (vector EcoRI site at the 5′ side of the insert) was digested with EcoRI for insertion of the 5′ cDNA fragment. This 5′ fragment was obtained by PCR amplification from the two-hybrid cDNA library with oligonucleotides 5′AD and 5′-CTTCTACCACAAACCGACGTCGTACCG-3′ and cloned into vector pCR 2.1 (Invitrogen, Carlsbad, CA). After sequencing, the 5′ insert was reisolated by digestion with EcoRI and subsequently ligated to the 3′ end of *AtPP2CA* cDNA in pBluescript KS+ vector.

Production of the AtPP2CA Interaction Domain in *E. coli*

The *AtPP2CA* insert obtained from the cDNA library (in vector pGAD10) was isolated by SalI digestion and then cloned into vector pET28c(+) (Novagen, Madison, WI) using the same restriction site. *E. coli* BL21(DE3) transformed with this construct (250 mL) was grown until the exponential phase was reached (OD = 0.6), and isopropylthio-β-galactoside (300 μM) was added to the culture. After 3 hr, cells were pelleted and frozen in liquid nitrogen. The pellet was treated as described in the Qiaexpressionist protocol (Qiagen, Valencia, CA). Extraction was performed under native conditions after resuspension in 2.5 mL of lysis buffer (50 mM Na phosphate buffer, pH 8, containing 300 mM NaCl and 10 mM imidazole).

Production of AKT2-CT in *Sf9* Cells

The AKT2 C-terminal domain (from amino acid 324 to the end) was cloned into vector pGmAc34T (Davrinche et al., 1993). *Sf*9 cell extracts were obtained as described by Daram et al. (1997). They were dialyzed for 2 hr against *Sf*9 buffer (50 mM Na phosphate buffer, pH 8, 150 mM NaCl, 10% glycerol, 1 mM phenylmethylsulfonyl fluoride, and 7 mM β-mercaptoethanol) containing 5 mM imidazole.

In Vitro Binding of AKT2-CT to AtPP2CA

A modified version of the Qiaexpressionist protocol (Qiagen) was used. A nickel–nitrilotriacetic acid agarose gel (0.3 mL of a 50% solution, washed with lysis buffer) was incubated for 1 hr with 1.25 mL of bacterial lysate containing His-tagged AtPP2CA. A column was obtained by pouring this mixture into a 1-mL pipette tip blocked with glass wool. A control column was prepared with the same amount of nickel–nitrilotriacetic acid agarose, which either had not been incubated with the bacterial lysate or had been incubated with bacterial extract from *E. coli* BL21 transformed with empty pET28c(+) vector. Both columns were treated in parallel.

They were washed with 2 × 1 mL of wash buffer and 1 mL of 50 mM Na phosphate buffer, pH 8. The dialyzed *Sf*9 cell extract, prepared from AKT2-CT–expressing cells as described above (0.5 mL per column, 3.5 mg of protein), then was loaded, and the flow-through was loaded a second time. Columns were washed twice with 1 mL of *Sf*9 buffer supplemented with 20 mM imidazole. Proteins were eluted with 250 mM imidazole in *Sf*9 buffer (3 × 170 μL). After SDS-PAGE (10% acrylamide), protein gel blot analysis was performed using the Aurora kit (ICN, Costa Mesa, CA) and a polyclonal antiserum raised against AKT2-CT. This antiserum was prepared using AKT2-CT expressed in *E. coli* as inclusion bodies and was purified by successive washes of the pellet and SDS-PAGE. The absence of cross-reaction with proteins from *Sf*9 cells infected with wild-type baculovirus was verified.

Localization of Promoter Expression Using β-Glucuronidase as a Reporter Gene

The *AtPP2CA* promoter region (3 kb) was amplified by PCR from an *Arabidopsis thaliana* (cv Wassilewskija) genomic DNA preparation with *pfu* DNA polymerase using oligonucleotides 5′-GGAGAAGCGCCGAATTCGAGTCATGG-3′ and 5′-CCCAGCCATGGGATCTCTAACAAAACTTC-3′. This fragment was digested with NcoI (partial) and EcoRI and inserted into pBI320.X (provided by R. Derose, Institute of Plant Molecular Biology, Strasbourg, France), leading to a fusion between the *AtPP2CA* promoter and the β-glucuronidase (*GUS*) coding sequence. The resulting plasmid then was digested with EcoRI and SacI, and the isolated fragment containing the AtPP2CA promoter–GUS fusion was ligated into binary vector pMOG402 (provided by A. Hoekema, MOGEN International, Leiden, The Netherlands). All subsequent steps (plant transformation, GUS assay, and cross-sections of plant tissues) were performed as described previously (Pilot et al., 2001). The insertion of the promoter-GUS fusion into the plant genome was checked by PCR analysis.

RNA Gel Blot Analysis

RNAs were extracted and hybridized as described previously (Pilot et al., 2001). The ^{32}P-labeled probe was obtained by PCR amplification using oligonucleotides 5′-CCGGTTGATTCAACTTCTCGAGC-3′ and 5′-CTGAGGAGACTGCAATTCACATC-3′, which delineate an *AtPP2CA*-specific region (nucleotides 49 to 648) at the beginning of the open reading frame.

PCR Experiments

Plants were grown for 4 weeks in a growth chamber (8 hr of light at 22°C, 16 hr of darkness at 20°C, RH of 70%) for an optimal develop-

ment of rosette leaves, then they were transferred for 24 hr in the greenhouse.

Mesophyll protoplasts were prepared as follows (protocol from E. Hosy, personal communication). Abaxial epidermal strips from large leaves were peeled, and epidermis-free areas were cut and digested in a solution containing 5 mM Mes-KOH, pH 5.5, 1 mM $CaCl_2$, 500 mM sorbitol, 2 mM ascorbic acid, 1% (w/v) cellulase, and 0.1% (w/v) pectolyase for 15 min at 27°C. The digestion mixture was filtered on nylon (0.05-mm mesh). The filtrate was recovered and diluted in enzyme-free digestion solution supplemented with 10 mM KCl. The mesophyll protoplast preparation was checked with a microscope for the absence of contaminating cells. The protoplast suspension was allowed to decant in a tube at 0°C, and the resulting pellet was frozen in liquid nitrogen until RNA extraction. Intact leaves of the same plants were harvested and frozen in liquid nitrogen.

RNAs from mesophyll protoplasts and whole leaves were extracted as described previously (Pilot et al., 2001). First-strand DNA synthesis was performed using Moloney murine leukemia virus reverse transcriptase (Promega) with 6 μg of total RNA and 10 pmole of oligo(dT)20 (final volume of 20 μL). The reaction medium was diluted 10-fold in water, and 5 μL was used for each PCR cycle (50 μL). Each couple of primers was chosen so as to surround at least one intron. The elongation factor 1α gene (*EF1α*) (Axelos et al., 1989) was used as a control. Primers were as follows: 5′-CCGGTTGATTCAACTTCTCGAGC-3′ and 5′-CTGAGGAGACTGCAATTCACATC-3′ for *AtPP2CA*; 5′-GCATTGAAGCAGCGTCAAACTTTGTTAACAG-3′ and 5′-CTTATGTGGATGTTGCAACCGTGC-3′ for *AKT2*; 5′-GACGCGATTTTCATCATCGACAAC-3′ and 5′-GGTTCGGCTAGTCCAATGAACGACGAGGTTGG-3′ for *KAT1*; 5′-GCCTTCATCACCTACAAGAAAG-3′ and 5′-CCGTGAAATAGGTAGACGTTCTGAACGATTGGG-3′ for *KAT2*; and 5′-CCACCACTGGTGGTTTTGAGGCTGGTATC-3′ and 5′-CATTGAACCCAACGTTGTCACCTGGAAG-3′ for *EF1α*. The reaction was stopped after 36 cycles, and an aliquot was loaded onto a 2% agarose gel.

cDNA Mutagenesis

The Altered Sites II In Vitro Mutagenesis System kit (Promega) was used. The 0.6-kb EcoRI-XbaI internal fragment of *AtPP2CA* cDNA was cloned into vector pAlter. Second-strand synthesis was performed with mutagenic oligonucleotide 5′-CATCATTTCTACGACGTCTTTGACGGC-3′, which was designed to create a G139D mutation and an AatII site by replacement of the GGTGTC sequence (amino acids Gly and Val) with GACGTC (amino acids Asp and Val). A clone was selected on the basis of the AatII restriction pattern. The native AatII internal site of *AtPP2CA* cDNA (not created by mutagenesis) was cut by partial digestion, and then complete NcoI digestion was performed to generate a 108-bp fragment. This fragment was ligated into *AtPP2CA* cDNA digested with AatII and NcoI. The entire region encompassing the 108-bp inserted fragment was verified by DNA sequencing.

Expression in COS Cells

Full-length cDNAs were cloned in pCI (Promega) or pIRES (Reyes et al., 1998), which is a pCI-derived vector that allows coexpression of the cDNA insert with a sequence encoding the membrane protein CD8 (providing a transfection marker). COS-7 cells were cultured in 2 mL of Dulbecco's modified Eagle's medium (Gibco BRL) supplemented with 10% fetal bovine serum (Gibco BRL) at 37°C in 5% CO_2. One day before transfection, cells were detached with trypsin-EDTA (Gibco BRL) and transferred to 35-mm dishes (20,000 cells per dish). For one transfection, 80 μL of HBS 2x (280 mM NaCl, 50 mM Hepes, and 15 mM Na_2HPO_4, pH 7.15) were mixed gently with 80 μL of TE-$CaCl_2$ (10 mM Tris, pH 8, 1 mM EDTA, and 250 mM $CaCl_2$) containing 0.75 μg of pCI-AKT2 plus 1.5 μg of cotransfection plasmid: pIRES-AtPP2CA or pIRES-AtPP2CA* (null G139D mutation), or empty pIRES. The DNA precipitate that was formed was spread onto cells in the culture medium.

After 8 hr, cells were rinsed twice with Dulbecco's modified Eagle's medium. Electrophysiological analyses were performed 3 days later. Transfected cells were detected with the anti-CD8 coated beads method (Jurman et al., 1994). The bath solution contained 150 mM KCl, 1 mM $CaCl_2$, 1.5 mM $MgCl_2$, and 10 mM Hepes/NaOH, pH 7.4. The pipettes (Kimax 51; Kimble Glass, Inc., Owens, IL) were filled with 150 mM KCl, 1.5 mM $MgCl_2$, 3 mM EGTA, 2.5 mM MgATP, and 10 mM Hepes/NaOH, pH 7.2. In the whole-cell configuration (Hamill et al., 1981), pulses of 1.6 sec were applied, from +40 to −160 mV with a holding potential of +40 mV (steps of 20 mV). Electrical signals were amplified by Axopatch 200 A (CV-201 A, software Clampex-6; Axon Instruments, Union City, CA). Control electrophysiological recordings in media supplemented with 10 mM CsCl were performed systematically (Cs^+ controls), as described previously (Lacombe et al., 2000), to check that the recorded current essentially flowed through K^+-selective channels (AKT2) and not through a nonselective leak pathway.

Expression in *Xenopus laevis* oocytes

Xenopus laevis (Centre de Recherche de Biochimie Macromoléculaire, Centre National de la Recherche Scientifique, Montpellier, France) oocytes were injected with 20 ng (0.02 μL) of pCI-AKT2, either alone or together with 40 ng of pCI-AtPP2CA. Control oocytes were injected with 0.02 μL of deionized water. Two-electrode voltage-clamp experiments were performed as described previously (Véry et al., 1995; Lacombe and Thibaud, 1998).

The standard external solution contained 20 mM KCl, 80 mM NaCl, 1.5 mM $CaCl_2$, 3 mM $MgCl_2$, and 10 mM Hepes/NaOH, pH 7.5. Vanadate is used classically at millimolar concentrations in the external solution to inhibit phosphatase activities in oocyte experiments (McNicholas et al., 1994; Becq et al., 1997; Tsai et al., 1999). To obtain the 3 mM (theoretical) vanadate external solution, sodium metavanadate (3 mM $NaVO_3$) was allowed to dissolve (strong magnetic stirring at 30°C) in the standard external solution for a few hours before the experiments. Oocytes were subjected to a first voltage clamp experiment (protocol: 1.6-sec pulses from +30 to −150 mV, in 20-mV steps, and a holding potential of −30 mV). Thereafter, the oocytes were treated with the vanadate external solution for 1.5 hr and subjected to a second voltage-clamp experiment (same protocol).

Cs^+ control recordings (see above for COS cells) were performed systematically before and after vanadate treatment to ensure that currents were generated by a potassium-selective channel.

Accession Numbers

The accession numbers for the sequences mentioned in this article are Z83202 (AtKC1), GI8778547 (ABI1), GI9759243 (ABI2), and GI39980397 (AtPP2C-HA).

ACKNOWLEDGMENTS

We are grateful to Nicole Grignon for assistance with microscopy techniques, to Eric Hosy for the protocol of mesophyll protoplast preparation, and to Isabel Lefevre for critical reading of the manuscript.

Received December 7, 2001; accepted February 18, 2002.

REFERENCES

Ache, P., Becker, D., Ivashikina, N., Dietrich, P., Roelfsema, M.R.G., and Hedrich, R. (2000). GORK, a delayed outward rectifier expressed in guard cells of *Arabidopsis thaliana*, is a K^+-selective, K^+-sensing ion channel. FEBS Lett. **486,** 93–98.

Ache, P., Becker, D., Deeken, R., Dreyer, I., Weber, H., Fromm, J., and Hedrich, R. (2001). VFK1, a *Vicia faba* K^+ channel involved in phloem unloading. Plant J. **27,** 571–580.

Allen, J.B., Walberg, M.W., Edwards, M.C., and Elledge, S.J. (1995). Finding prospective partners in the library: The two-hybrid system and phage display find a match. Trends Biochem. Sci. **20,** 511–516.

Armstrong, F., Leung, J., Grabov, A., Brearley, J., Giraudat, J., and Blatt, M.R. (1995). Sensitivity to abscisic acid of guard-cell K^+ channel is suppressed by abi1-1, a mutant Arabidopsis gene encoding a putative protein phosphatase. Proc. Natl. Acad. Sci. USA **92,** 9520–9524.

Axelos, M., Bardet, C., Liboz, T., Le Van Thai, A., Curie, C., and Lescure, B. (1989). The gene family encoding the *Arabidopsis thaliana* translation elongation factor EF-1α: Molecular cloning, characterization and expression. Mol. Gen. Genet. **219,** 106–112.

Baizabal-Aguirre, M., Clemens, S., Uozumi, N., and Schroeder, J.I. (1999). Suppression of inward-rectifying K^+ channels KAT1 and AKT2 by dominant negative point mutations in the KAT1 α-subunits. J. Membr. Biol. **167,** 119–125.

Bartel, P.L., and Fields, S. (1995). Analyzing protein-protein interactions using two-hybrid system. Methods Enzymol. **254,** 241–263.

Becq, F., Hamon, Y., Bajetto, A., Gola, M., Verrier, B., and Chimini, G. (1997). ABC1, an ATP binding cassette transporter required for phagocytosis of apoptotic cells, generates a regulated anion flux after expression in *Xenopus laevis* oocytes. J. Biol. Chem. **272,** 2695–2699.

Blatt, M.R. (1992). K^+ channels of stomatal guard cells. J. Gen. Physiol. **99,** 615–644.

Blatt, M.R. (2000). Cellular signaling and volume control in stomatal movements in plants. Annu. Rev. Cell Dev. Biol. **16,** 221–241.

Bockenhauer, D., Zilberberg, N., and Goldstein, S.A.N. (2001). KCNK2: Reversible conversion of a hippocampal potassium leak into a voltage-dependent channel. Nat. Neurosci. **4,** 1–6.

Booij, P.P., Roberts, M.R., Vogelzang, S.A., Kraayenhof, R., and de Boer, A.H. (1999). 14.3.3. proteins double the number of outwardly-rectifying K^+ channels available for activation in tomato cells. Plant J. **20,** 673–683.

Cao, Y., Ward, J.M., Kelly, W.B., Ichida, A.M., Gaber, R.F., Anderson, J.A., Uozumi, N., Schroeder, J.I., and Crawford, N.M. (1995). Multiple genes, tissue specificity, and expression-dependent modulation contribute to the functional diversity of potassium channels in *Arabidopsis thaliana*. Plant Physiol. **109,** 1093–1106.

Daram, P., Urbach, S., Gaymard, F., Sentenac, H., and Chérel, I. (1997). Tetramerization of the AKT1 plant potassium channel involves its C-terminal cytoplasmic domain. EMBO J. **16,** 3455–3463.

Davrinche, C., Pasquier, C., Cerutti, M., Serradell, L., Clément, D., Devauchelle, G., Michelson, S., and Davignon, J.L. (1993). Expression of human cytomegalovirus immediate early protein IE1 in insect cells: Splicing of RNA and recognition by $CD4^+$ T-cell clones. Biochem. Biophys. Res. Commun. **195,** 469–477.

Deeken, R., Sanders, C., Ache, P., and Hedrich, R. (2000). Developmental and light-dependent regulation of a phloem-localised K^+ channel of *Arabidopsis thaliana*. Plant J. **23,** 285–290.

Delrot, S., and Bonnemain, J.L. (1985). Mechanism and control of phloem transport. Physiol. Veg. **23,** 199–220.

Dennison, K.L., Robertson, W.R., Lewis, B.D., Hirsch, R.E., Sussman, M.R., and Spalding, E.P. (2001). Functions of AKT1 and AKT2 potassium channels determined by studies of single and double mutants of *Arabidopsis*. Plant Physiol. **127,** 1012–1019.

Dreyer, I., Michard, E., Lacombe, B., and Thibaud, J.B. (2001). A plant Shaker-like K^+ channel switches between two gating modes resulting in either inward-rectifying or "leak" current. FEBS Lett. **505,** 233–239.

Felle, H.H., Hanstein, S., Steinmeyer, R., and Hedrich, R. (2000). Dynamics of ionic activities in the apoplast of the sub-stomatal cavity of intact *Vicia faba* leaves during stomatal closure evoked by ABA and darkness. Plant J. **24,** 297–304.

Fromm, J., and Bauer, T. (1994). Action potentials in maize sieve tubes change phloem translocation. J. Exp. Bot. **45,** 463–469.

Gaymard, F., Pilot, G., Lacombe, B., Bouchez, D., Bruneau, D., Boucherez, J., Michaux-Ferrière, N., Thibaud, J.B., and Sentenac, H. (1998). Identification and disruption of a plant shaker-like channel involved in K^+ release into the xylem sap. Cell **94,** 647–655.

Gietz, D., St. Jean, A., Woods, R.A., and Schiestl, R.H. (1992). Improved method for high efficiency transformation of intact yeast cells. Nucleic Acids Res. **20,** 1425.

Gosti, F., Bertauche, N., Vartanian, N., and Giraudat, J. (1995). Abscisic acid-dependent and -independent regulation of gene expression by progressive drought in *Arabidopsis thaliana*. Mol. Gen. Genet. **246,** 10–18.

Gosti, F., Beaudoin, N., Serizet, C., Webb, A.A.R., Vartanian, N., and Giraudat, J. (1999). ABI1 protein phosphatase 2C is a negative regulator of abscisic acid signaling. Plant Cell **11,** 1897–1909.

Hamill, O.P., Marty, A., Neher, E., Sakmann, B., and Sigworth, F.J. (1981). Improved patch-clamp techniques for high-resolution current recording from cells and cell-free membrane patches. Pflugers Arch. **391,** 85–100.

Hirsch, R.E., Lewis, B.D., Spalding, E.P., and Sussman, M.R. (1998). A role for the AKT1 potassium channel in plant nutrition. Science **8,** 918–921.

Hoshi, T. (1995). Regulation of voltage dependence of the KAT1 channel by intracellular factors. J. Gen. Physiol. **105,** 309–328.

Hwang, J.U., Suh, S., Kim, J., and Lee, Y. (1997). Actin filaments modulate both stomatal opening and inward K^+ channel activities in guard cells of *Vicia faba*. Plant Physiol. **115,** 335–342.

Ichida, A.M., Pei, Z.M., Baizabal-Aguirre, V.M., Turner, K.J., and Schroeder, J.I. (1997). Expression of a Cs(+)-resistant guard cell K^+ channel confers Cs(+)-resistant, light-induced stomatal opening in transgenic Arabidopsis. Plant Cell **9,** 1843–1857.

Jurman, M.E., Boland, L.M., Liu, Y., and Yellen, G. (1994). Visual identification of individual transfected cells for electrophysiology using antibody-coated beads. Biotechniques **17,** 876–881.

Kochian, L.V., and Lucas, W.J. (1988). Potassium transport in roots. Adv. Bot. Res. **15,** 93–178.

Kuromori, T., and Yamamoto, M. (1994). Cloning of cDNAs from *Arabidopsis thaliana* that encode putative protein phosphatase 2C and a human Dr1-like protein by transformation of a fission yeast mutant. Nucleic Acids Res. **22,** 5296–5301.

Lacombe, B., and Thibaud, J.B. (1998). Evidence for a multi-ion behavior in the plant potassium channel KAT1. J. Membr. Biol. **166,** 91–100.

Lacombe, B., Pilot, G., Michard, E., Gaymard, F., Sentenac, H., and Thibaud, J.B. (2000). A shaker-like K^+ channel with weak rectification is expressed in both source and sink phloem tissues of Arabidopsis. Plant Cell **12,** 837–851.

Lagarde, D., Basset, M., Lepetit, M., Conejero, G., Gaymard, F., Astruc, S., and Grignon, C. (1996). Tissue-specific expression of Arabidopsis *AKT1* gene is consistent with a role in K^+ nutrition. Plant J. **9,** 195–203.

Leonhardt, N., Marin, E., Vavasseur, A., and Forestier, C. (1997). Evidence for the existence of a sulfonylurea-receptor-like protein in plants: Modulation of stomatal movements and guard cell potassium channels by sulfonylureas and potassium channel openers. Proc. Natl. Acad. Sci. USA **94,** 14156–14161.

Lesage, F., and Lazdunski, M. (2000). Molecular and functional properties of two-pore-domain potassium channels. Am. J. Physiol. **279,** F793–F801.

Leung, J., and Giraudat, J. (1998). Abscisic acid signal transduction. Annu. Rev. Plant Physiol. **49,** 199–222.

Leung, J., Merlot, S., and Giraudat, J. (1997). The Arabidopsis ABSCISIC ACID-INSENSITIVE2 (ABI2) and ABI1 genes encode homologous protein phosphatases 2C involved in abscisic acid signal transduction. Plant Cell **9,** 759–771.

Leyman, B., Geelen, D., Quintero, F., and Blatt, M.R. (1999). A tobacco syntaxin with a role in hormonal control of guard cell ion channels. Science **283,** 537–540.

Li, J., Lee, Y.R.J., and Assmann, S.M. (1998). Guard cells possess a calcium-dependent protein kinase that phosphorylates the KAT1 potassium channel. Plant Physiol. **116,** 785–795.

Li, W., Luan, S., Schreiber, S.L., and Assmann, S. (1994). Evidence for protein phosphatase 1 and 2A regulation of K^+ channels in two types of leaf cells. Plant Physiol. **106,** 963–970.

Maathuis, F.J.M., and Sanders, D. (1995). Contrasting roles in ion transport of two K^+-channel types in root cells of *Arabidopsis thaliana*. Planta **197,** 456–464.

Marten, I., Hoth, S., Deeken, R., Ache, P., Ketchum, K., Hoshi, T., and Hedrich, R. (1999). AKT3, a phloem-localised K^+ channel, is blocked by protons. Proc. Natl. Acad. Sci. USA **96,** 7581–7586.

McNicholas, C.M., Wang, W., Ho, K., Hebert, S., and Giebisch, G. (1994). Regulation of ROMK1 K^+ channel activity involves phosphorylation processes. Proc. Natl. Acad. Sci. USA **91,** 8077–8081.

Merlot, S., Gosti, F., Guerrier, D., Vavasseur, A., and Giraudat, J. (2001). The ABI1 and ABI2 protein phosphatases 2C act in a negative feedback regulatory loop of the abscisic acid signalling pathway. Plant J. **25,** 1–10.

Mori, I.C., Uozumi, N., and Muto, S. (2000). Phosphorylation of the inward-rectifying potassium channel KAT1 by ABR kinase in *Vicia* guard cells. Plant Cell Physiol. **41,** 850–856.

Nakamura, R.L., McKendree, W.L., Jr., Hirsch, R.E., Sedbrook, J.C., Gaber, R.F., and Sussman, M.R. (1995). Expression of an *Arabidopsis* potassium channel gene in guard cells. Plant Physiol. **109,** 371–374.

Pei, Z.M., Kuchitsu, K., Ward, J.M., Schwartz, M., and Schroeder, J.I. (1997). Differential abscisic acid regulation of guard cell slow anion channels in Arabidopsis wild-type and abi1 and abi2 mutants. Plant Cell **9,** 409–423.

Philippar, K., Fuchs, I., Luthen, H., Hoth, S., Bauer, C.S., Haga, K., Thiel, G., Ljung, K., Sandberg, G., Bottger, M., Becker, D., and Hedrich, R. (1999). Auxin-induced K^+ channel expression represents an essential step in coleoptile growth and gravitropism. Proc. Natl. Acad. Sci. USA **96,** 12186–12191.

Pilot, G., Lacombe, B., Gaymard, F., Chérel, I., Boucherez, J., Thibaud, J.B., and Sentenac, H. (2001). Guard cell inward K^+ channel activity in *Arabidopsis* involves expression of the twin channel subunits KAT1 and KAT2. J. Biol. Chem. **276,** 3215–3221.

Reyes, R., Duprat, F., Lesage, F., Fink, M., Salinas, M., Farman, N., and Lazdunski, M. (1998). Cloning and expression of a novel pH-sensitive two pore domain K^+ channel from human kidney. J. Biol. Chem. **273,** 30863–30869.

Rodriguez, P.L. (1998). Protein phosphatase 2C (PP2C) function in higher plants. Plant Mol. Biol. **38,** 919–927.

Saalbach, G., Schwerdel, M., Natura, G., Buschmann, P., Christov, V., and Dahse, I. (1997). Over-expression of the plant 14.3.3 proteins in tobacco: Enhancement of the plasmalemma K^+ conductance of mesophyll cells. FEBS Lett. **413,** 294–298.

Schroeder, J., Ward, J.M., and Gassmann, W. (1994). Perspectives on the physiology and structure of inward-rectifying K^+ channels in higher plants: Biophysical implications for K^+ uptake. Annu. Rev. Biophys. Biomol. Struct. **23,** 441–471.

Sheen, J. (1998). Mutational analysis of protein phosphatase 2C involved in abscisic acid signal transduction in higher plants. Proc. Natl. Acad. Sci. USA **95,** 975–980.

Sotta, B., Sossountzov, L., Maldiney, R., Sabbagh, I., Tachon, P., and Miginiac, E. (1985). Abscisic acid localization by light microscopic immunohistochemistry in *Chenopodium polyspermum*: Effect of water stress. J. Histochem. Cytochem. **33,** 201–208.

Spalding, E., and Goldsmith, M.H.M. (1993). Activation of K^+ channels in the plasma membrane of Arabidopsis by ATP produced photosynthetically. Plant Cell **5,** 477–484.

Szyroki, A., Ivashikina, N., Dietrich, P., Roelfsema, M.R.G., Ache, P., Reintanz, B., Deeken, R., Godde, M., Felle, H., Steinmeyer, R., Palme, K., and Hedrich, R. (2001). KAT1 is not essential for stomatal opening. Proc. Natl. Acad. Sci. USA **98,** 2917–2921.

Tähtiharju, S., and Palva, T. (2001). Antisense inhibition of protein phosphatase 2C accelerates cold acclimation in *Arabidopsis thaliana*. Plant J. **26,** 461–470.

Tang, H., Vasconcelos, A.C., and Berkowitz, G.A. (1996). Physical association of KAB1 with plant K^+ channel alpha subunits. Plant Cell **8,** 1545–1553.

Tang, X.D., and Hoshi, T. (1999). Rundown of the hyperpolarization-activated KAT1 channel involves slowing of the opening transitions regulated by phosphorylation. Biophys. J. **76,** 3089–3098.

Thiel, G., MacRobbie, E.A., and Blatt, M.R. (1992). Membrane transport in stomatal guard cells: The importance of voltage control. J. Membr. Biol. **126,** 1–18.

Travis, S.M., Berger, H.A., and Welsh, M.J. (1997). Protein phosphatase 2C dephosphorylates and inactivates cystic fibrosis transmembrane conductance regulator. Proc. Natl. Acad. Sci. USA **94,** 11055–11060.

Tsai, W., Morielli, A.D., Cachero, T.G., and Peralta, E.G. (1999). Receptor protein tyrosine phosphatase α participates in the m1 muscarinic acetylcholine receptor-dependent regulation of Kv1.2 channel activity. EMBO J. **18,** 109–118.

Urbach, S., Chérel, I., Sentenac, H., and Gaymard, F. (2000). Biochemical characterization of the *Arabidopsis* K^+ channels KAT1 and AKT1 expressed or co-expressed in insect cells. Plant J. **23,** 527–538.

Véry, A.A., Gaymard, F., Bosseux, C., Sentenac, H., and Thibaud, J.B. (1995). Expression of a cloned plant K^+ channel in *Xenopus* oocytes: Analysis of macroscopic currents. Plant J. **7,** 321–332.

Vranova, E., Tähtiharju, S., Sriprang, R., Willekens, H., Heino, P., Palva, E.T., Inzé, D., and Van Camp, W.V. (2001). The AKT3 potassium channel protein interacts with the AtPP2CA protein phosphatase 2C. J. Exp. Bot. **52,** 181–182.

Vreugdenhil, D. (1985). Source-to-sink gradient of potassium in the phloem. Planta **211,** 105–111.

Wang, X.Q., Hemayet, U., Jones, A.M., and Assmann, S.M. (2001). G protein regulation of ion channels and abscisic acid signaling in Arabidopsis guard cells. Science **292,** 2070–2072.

Wu, W.H., and Assmann, S.M. (1994). A membrane-delimited G protein regulation of the guard-cell inward K^+ channel. Proc. Natl. Acad. Sci. USA **91,** 6310–6314.

Zhang, X., Ma, J., and Berkowitz, G.A. (1999). Evaluation of functional interaction between K^+ channel α- and β-subunits and putative inactivation gating by co-expression in *Xenopus laevi*s oocytes. Plant Physiol. **121,** 995–1002.